Ultra-high resolution optical vector analysis based on Optical double sideband modulation

WANG Wenyu*[a], ZHOU Jing[a], YU Changyuan[a]
[a]Dept. of Eletrical and Electronic Engneering, The Hong Kong Polytechnic University, 11 Yuk Choi Rd, Hung Hom, Hong Kong, PR China.

ABSTRACT

Microwave photonics is an interdisciplinary research field that combines the fields of optics and radio frequency. The main functions of microwave photonic systems include photon generation, processing, control and distribution of microwave and millimeter wave (mm-wave) signals. Because of its combined advantages of optics and radio frequency, it is used in applications such as broadband wireless access networks, sensor networks, radar, satellite communications, instrumentation, and warfare systems. This article reviews the development and applications of microwave photonics, providing an overview of photon generation of microwave and millimeter-wave signals, photon processing of microwave and millimeter-wave signals, photon-assisted microwave measurements, fiber-optic radio systems, and integrated microwave photonics. Among them, the optical vector analysis (OVA) technology in Microwave spectrum analysis is analyzed from the principles, development status, structural examples and other aspects, and the OVA based on optical double sideband (ODSB) modulation is studied and simulated in detail. And the performance of the ODSB-based OVA is improved by using the measurement range broadening technology based on optical frequency comb, the measurement error elimination technology based on carrier suppression and balanced photoelectric detection, and the linearly frequency modulation (LFM)-based OVA.

Keywords: Microwave photonics, optical vector analysis, double sideband modulation, linearly frequency modulation

1. INTRODUCTION

In recent years, photonics utilizes the ultra-wide bandwidth of the high carrier frequency of light to achieve optical communication, which can provide ultra-high transmission capacity and a wide transmission range. However, in the face of the current explosive growth of transmitted information, ultra-high requirements on spectrum utilization and the development of optical technology have led to the excessive use of narrowband optical devices. The new generation of optical information systems (optical communications, optical sensing, optical processing, etc.) urgently needs photonic devices that can perform multi-dimensional (amplitude, phase, polarization, etc.) and high-precision control of broadband spectrum. Therefore, accurate measurement of the multidimensional spectral response of these photonic devices has become a prerequisite for innovation and breakthroughs in related fields.

Measurement and analysis are critical in the development and manufacturing of high-performance optical components and communication systems. Some design and manufacturing problems can be discovered by measuring several key parameters, but currently no light vector analysis instrument has been manufactured at home or abroad that can measure the spectral response of optical devices with femtometer-level spectral accuracy. Therefore, in order to achieve

Optoelectronic Devices and Integration XIII, edited by Xuping Zhang, Baojun Li, Changyuan Yu, Xinliang Zhang, Proc. of SPIE Vol. 13236, 1323609
 · 0277-786X · doi: 10.1117/12.3034487

high-resolution optical vector analysis, researchers proposed and established an optical vector analyzer based on microwave photonics (MWP). [1-4] Among them, electro-optical conversion is used to convert the frequency scan in the electrical domain to the optical domain to improve the measurement resolution. Benefiting from high-resolution electrical sweeps, MWP-based OVA theoretically has sub-hertz resolution (334Hz).

With the in-depth study of microwave photonics, applications based on microwave photonics have gradually come into view and become a current research hotspot. They can be roughly divided into four categories: 1. Microwave photonic signal processing: The essence of the microwave photonic signal processor is a photonic system whose main purpose is to benchmark ordinary microwave filters in radio frequency systems and perform the same tasks with the introduction of complementary benefits inherent in photonics. Usually, using devices based on free space optics, integrated optics, and fiber optics, the following microwave signal processing functions can be implemented in the optical domain: filtering, arbitrary waveform generation, beam control, analog-to-digital conversion, and frequency measurement. [5-11] 2. Photonic for microwave measurements: Among the complementary benefits and many functions achieved by photonics, photonics-based microwave measurement can bring excellent performance, such as large instantaneous bandwidth, wide frequency coverage and strong immunity to electromagnetic interference (EMI). With the development of photonic microwave measurement technology, researchers have proposed many systems based on basic system architecture. The most important ones are recent advances in photonic microwave spectrum analysis and photonic instantaneous frequency measurement (IFM).[12-17] 3. High speed mm-wave and radio-over-fiber (ROF) systems: Optical fiber communication brings the advantages of long transmission distance, large frequency bandwidth, and strong anti-interference ability to traditional radio communication technology. In recent years, with the explosive growth of network data, many different millimeter wave fiber optic radio solution strategies are being investigated to meet future multi-gigabit wireless data transmission needs.[18] 4. Integrated microwave photonics: Integrated MWP is an emerging field of scientific and technological research based on the rise of microwave photonic technology and photonic integration technology. The aim is to integrate MWP components/subsystems into photonic circuits, considered critical to enable low-cost and advanced analog optical front ends[19], and emerging materials and significant advances in chip hybrid integration have allowed all key components of an integrated microwave photonic system to be integrated into a single chip. These advances not only equip microwave photonics with advanced capabilities but also greatly expand the scope and performance of the field. Its advanced technology can be intersected with a variety of emerging technologies, involving quantum, mechanics, neural networks, and other fields, driving new phases beyond telecommunications-related applications.[20]

In this article, we introduced the the OVA technology in Microwave spectrum analysis in detail, and the OVA based on double sideband modulation is studied and simulated in detail. And the performance of the ODSB-based OVA is improved by using the measurement range broadening technology based on optical frequency comb, the measurement error elimination technology based on carrier suppression and balanced photoelectric detection, and the LFM-based OVA.

2. METHODOLOGY

Optical devices are the cornerstone of a new generation of optical information systems (optical communications, optical sensing, optical processing, quantum computing, etc). Optical vector analysis technology is a basic measurement method for measuring the characteristics of optical devices. It can analyse optical devices from a multi-dimensional perspective,

which includes amplitude, phase, polarization response, etc. The principle of the optical vector analyzer is to use an optical signal with known parameters to pass through the device under test (DUT) and perform a linear frequency scan on it. Before the formal experiment begins, the system is calibrated, and the input signal is measured. Therefore, by comparing the omniscient signal and the signal with changed spectral component parameters after passing through the DUT, the frequency response of the DUT can be obtained. Then, combined with coherent detection technology, the Jones matrix of the DUT is derived, and then the optical parameters such as insertion loss, dispersion, polarization mode dispersion, and polarization-dependent loss of the device are obtained. Since the creation of the first model, OVA has been greatly improved, some new structures have been proposed with the accuracy has also improved. With the improvements, the difference in scanning signals becomes the essence, some of which are tunable single-frequency signals from laser sources, or optical single-sideband (OSSB) and optical double-sideband modulations from electro-optical modulators. Of course, regardless of the generation and characteristics of the input optical signal, it must eventually be converted into an electrical signal by a photodetector.

The researchers created an OVA based on optical double sideband (ODSB) modulation. There are many advantages: 1. Doubled measurement range, since the measurement range is limited by the maximum operating frequency of the electro-optical modulator, up to 80 GHz when using a component matrix based on lithium niobate (LiNbO3). 2. With an ultra-high resolution of approximately 667kHz, this is affected by the number of electrical measurement control points of the vector network analyzer. 3. Under certain circumstances, the measurement error caused by high-order sideband beats can be eliminated, which further relieves the limitation on the amplitude of the modulation index, thereby eliminating the limitation on the dynamic range. [14]

2.1 Classification of OVA based on ODSB

OVA based on ODSB is mainly divided into two methods: symmetric ODSB and asymmetric ODSB. The following figure 1 depicts the spectrum of the different scanning signal.

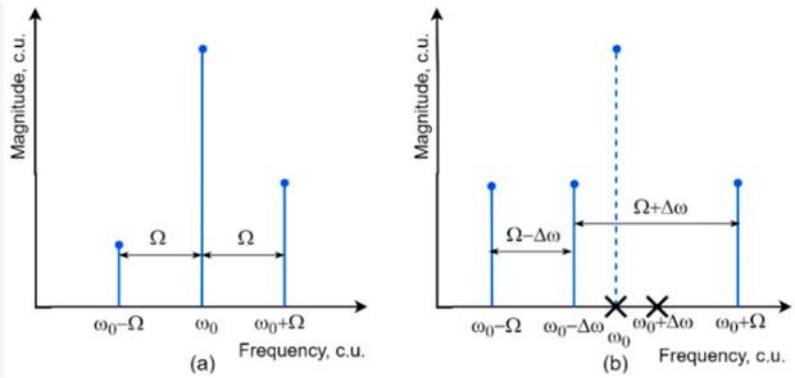

Figure 1. Spectra of scanning optical double-sideband (ODSB)-signals:(a)With symmetric ODSB,(b) with asymmetric ODSB.ω_0—the frequency of optical carrier; Ω—the modulation frequency; Δω—a fixed frequency shift

As we can see, the carrier is in the center of the studied spectrum, swept by the first-order sidebands on both sides of the spectrum. The advantages and shortcomings of the two forms are as follows: 1. For OVA with symmetrical ODSB, the process of get the frequency sweep signal is easy. But it requires two measurements to obtain result and have some difficulty in eliminating errors caused by higher-order sidebands. 2. For OVA with asymmetric ODSB, obtaining the scan

signal is not simple, but only one measurement is required, and there is no measurement error due to high-order sidebands. Thus, both approaches were developed simultaneously.

2.2 Principle of OVA based on ODSB

In this section, an ultra-high-resolution OVA based on ODSB will be constructed and studied. Figure 2 below depicts the general structure of the proposed ODSB-based OVA. Among them, the optical carrier generated from the laser source is modulated with a deterministic RF signal at the MZM modulator to complete the E/O conversion. Subsequently, the generated scanned ODSB signal passes through the DUT, where the amplitude and phase of the optical carrier and ±1st-order sidebands in the ODSB signal change according to the spectral response of the DUT. Next, the signal carrying the spectral response of the DUT is converted into photocurrent through the optical elements on the photoelectric conversion module. Finally, the amplitude and phase of the photocurrent are extracted using an electrical phase amplitude detector referenced by the RF signal to obtain the spectral response of the DUT.

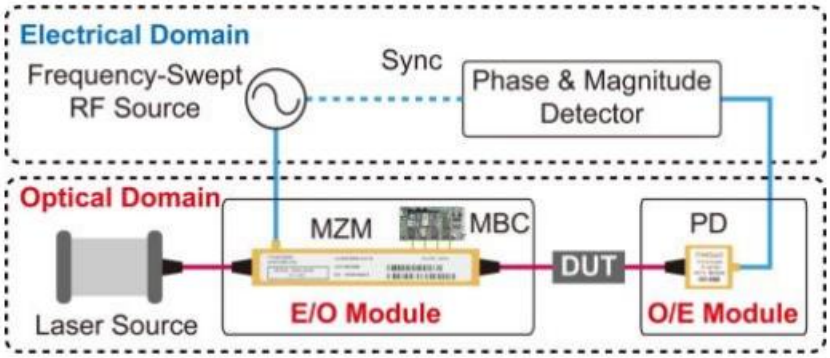

Figure 2. The structure of the OVA the proposed ODSB-based OVA.

Theoretically, when performing numerical calculations on small modulation situations, there are only the optical carrier and positive and negative first-order sidebands after the MZM modulator, so the optical field of the modulated signal can be expressed by the following formula: [21]

$$E_{MZM}(\omega) = a_{+1}A_n\delta[\omega - (\omega_0 + \omega_e)] + a_{-1}A_n\delta[\omega - (\omega_0 - \omega_e)] + a_0A_n\delta[\omega - \omega_0)]$$

where $a_{\pm1}$ and a_0 are the relative amplitudes of the sweeping ±lst order sidebands and the carrier, respectively. A_n is the complex amplitude of the n th-order sideband, ω_0 and ω_e are the angular frequencies of the optical carrier and the RF signal, respectively.

Next, the detection signal enters the measurement path, passes through the device under test. The optical signal carrying the spectral responses can be given by:

$$E_{out}(\omega) = H(\omega) * E_{MZM}(\omega) = a_{+1}A_n\mathrm{H}(\omega_0 + \omega_e)\delta[\omega - (\omega_0 + \omega_e)]$$
$$+a_{-1}A_n\mathrm{H}(\omega_0 - \omega_e)\delta[\omega - (\omega_0 - \omega_e))$$
$$+a_0A_n\mathrm{H}(\omega_0)\delta[\omega - \omega_0)]$$

Where $H(\omega)=H_{DUT}(\omega)*H_{SYS}(\omega)$, $H_{DUT}(\omega)$ and $H_{SYS}(\omega)$denote the transmission responses of the DUT and the measurement system.

This optical signal is then square-law detected in the PD (PD1), resulting in a photocurrent containing components in the sweeping sidebands, carrier, higher-order sidebands and other wavelength channels. The photocurrent generated after ±1 sideband and frequency-shifted carrier beat is

$$i_{MZM}(\omega_e) = \eta A_{+1} A_0^* H(\omega o + \omega e) H^*(\omega o) + \ \eta A0 A_{-1}^* H(\omega o) \times H^*(\omega o - \omega e)$$

where η is the responsivity of the PD.

Finally, we need to measure the interference produced by the system itself. Let $H_{DUT}(\omega) = 1$, that is, remove the component under test and directly connect the two measurement ports to get $H_{sys}(\omega)$:

$$i_{sys}(\omega_e) = \ \eta A_{+1} A_0^* H_{sys}(\omega o + \omega e) H_{sys}^*(\omega o) + \ \eta A0 A_{-1}^* H_{sys}(\omega o) \times H_{sys}^*(\omega o - \omega e)$$

Therefore, the transmission response of the component under test can be obtained as

$$H_{DUT}(\omega_0 + \omega_e) = \frac{i_{MZM}(\omega_e)}{i_{sys}(\omega_e) H_{DUT}^*(\omega_0)}$$

$$H_{DUT}(\omega_0 - \omega_e) = \frac{i_{MZM}^*(\omega_e)}{i_{sys}^*(\omega_e) H_{DUT}^*(\omega_0)}$$

Where $H_{DUT}(\omega_0)$ is the frequency response displayed by the DUT when the frequency is a constant value and can be expressed as a complex constant.

2.3 Research on measurement range broadening technology based on optical frequency comb

According to the theory, the measurement range of ODSB-based OVA has doubled. But it will still be limited by the bandwidth of microwave devices, electro-optical modulators, and photodetectors. Its measurement range is far from meeting the needs of photonic devices for hundreds of GHz or even THz measurement range. Broadband, high-resolution optical vector analysis will provide strong data support for the development, testing, production and application of current photonic devices and core photonic integrated chips with high-precision spectral control capabilities, further accelerating the research process.

One method is to exploit a tunable optical source to expand the measurement range. However, in actual measurements, the poor wavelength accuracy and stability of the tunable light source will cause the measurement resolution to deteriorate sharply. Therefore, a measurement range expansion technology based on optical frequency comb channelized measurement is proposed. Figure 3 illustrates the structure of the OVA using an optical frequency comb (OFC). [22]

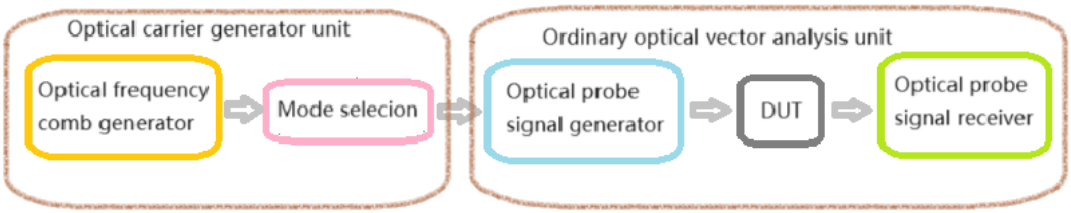

Figure 3. The structure of the OVA using an optical frequency comb.

The proposed system mainly contains of two parts: the optical carrier generation unit and the ordinary optical vector analysis unit. The optical carrier generation unit includes an OFC generator and mode selection. The optical signal

emitted by the ultra-narrow linewidth laser, and then goes through the OFC generator to get an ultra-narrow linewidth OFC signal. The mode selection is used to select the required comb line and transmit it to the OVA unit as an optical carrier. The OVA unit is mainly composed of optical probe signal generation module, DUT and optical probe signal receiver module. Among them, the optical probe signal generation module selects various electro-optical modulators according to different structures. These modulators will modulate the microwave signal output from the microwave sweep source onto the optical carrier output from the optical carrier generation unit, generate optical double-sideband signal and send it to the optical input port of the DUT. When propagated through the DUT, the amplitude and phase responses of the optical double-sideband signal carrier and sidebands change according to spectral response of the DUT. Then the signal enters the optical probe signal receiver module. The photodetector performs square-law detection on the optical signal, and the spectral information of the DUT carried is converted into the electrical domain. Signal processing is then performed to obtain the spectral response of the DUT.

Just use the module selection to select other comb lines and can measure the spectral response of the component under test in other sub-bands. Thanks to the high-precision comb line spacing of the optical frequency comb, when the measurement range of each sub-band is reasonably arranged without affecting the resolution, it is ensured that the measurement range of the optical vector analysis system is greater than the frequency spacing between the comb line of the optical frequency comb signal, can achieve seamless connection. Finally, by integrating the spectral responses of multiple adjacent sub-bands, a complete wide-bandwidth, high-resolution spectral response of the DUT can be obtained. And since the spectral response of the optical device to be tested in the overlapping area of adjacent sub-bands must be the same, the influence of the amplitude and phase differences of adjacent comb teeth of the optical frequency comb can be eliminated during spectrum integration. [23]

2.4 Nonlinear error analytical analysis, simulation and elimination on ultra-high-resolution OVA

One of the key links in ultra-high-resolution OVA is the use of electro-optical conversion to convert coarse light wavelength scanning into fine frequency scanning in the electrical domain. However, since the essence of electro-optical conversion is nonlinear processing, currently available electro-optical modulation (such as MZM in the previous section) must have nonlinear effects. In addition to generating the required first-order sidebands and optical carriers, a large number of unwanted higher-order sidebands are also mixed. The component beat by the high-order sideband is the same as the required information component captured by the first-order sideband and the frequency of the optical carrier, which will bring about measurement errors and further reduce the accuracy of measurement.[24]

In order to eliminate the unwanted signals caused by the high-order sidebands introduced by the nonlinear modulation of this electro-optical modulator, a nonlinear error elimination method based on carrier suppression and balanced photodetection is proposed. Figure 4 is a functional structure of an optical vector analysis system using this method. In this method, the optical signal propagating through the optical DUT is separated into two parts. One part is directly converted into a photocurrent containing information components and nonlinear errors, and the other is converted into a photocurrent containing only nonlinear errors after filtering out photocarriers. Make the two optical paths have the same length and insertion loss, and then conduct photoelectric detection of the two optical signals simultaneously. The two photocurrents are vectorially subtracted in balanced photodetector, and the nonlinear error of the photocurrent can be eliminated.

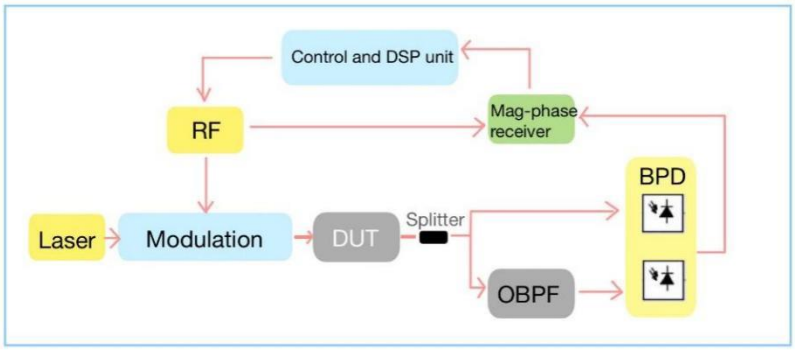

Figure 4. A functional block diagram of an OVA system based on carrier suppression and balanced photodetection

2.5 Ultra-high resolution optical vector analysis based on LFM (linearly frequency-modulation)

In practice experiments, the performance of measurement methods based on ODSB is limited by point-by-point microwave frequency sweep, thus the measurement speed is slow and difficult to improve. When faced with emergencies in advanced and emerging photonics and optical communications, it is difficult for ODSB-based measurement methods to achieve real-time monitoring. Therefore, measurement technology that combines ultra-high resolution and ultra-fast measurement speed is required.

In this section, OSSB-based OVA can be improved using electrical LFM signals. LFM signal has a large time-width-bandwidth product, can obtain a large pulse compression ratio, has the characteristics of long operating distance and high resolution. And in actual work, for example, using a large LFM rate (1600THz/s) in this article, the measurement of 16GHz bandwidth only takes 10 μs, and ultra-fast measurement can be completed.[25]

The bandwidth and duration of the LFM pulse signal can be selected by yourself., and are mutually restricted unlike the rectangular pulse signal. Since the frequency of the LFM signal grows linearly with time, the influence of nonlinear errors can be avoided. The system sets up a reference path and put the reference signal and probe signal into a balanced photodetector as shown in figure 5. While performing photoelectric conversion, the reference signal and the detection signal are mixed to perform de-chirp, and then undergo digital signal processing. In addition, the receiver only needs low-speed photodetector and ADC, because the wide-band LFM signal can be directly dechirped in the optical domain.

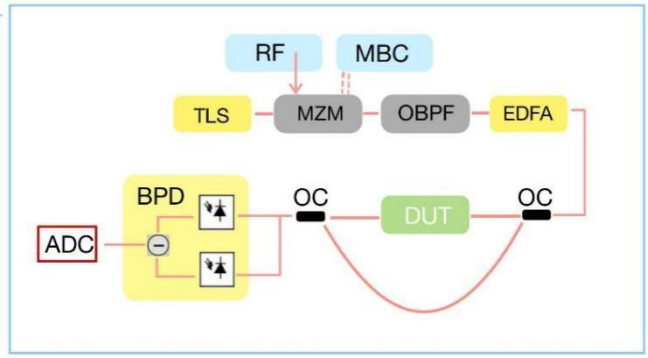

Figure 5. Schematic diagram of the proposed LFM-based OVA.TLS, tunable laser source; EDFA, erbium-doped fiber amplifier; OC, optical coupler; DUT, device under test; BPD, balanced photodetector; ADC, analog-to-digital converter; MZM,Mach-Zehnder modulator; OBPF, optical band-pass filter; MBC,modulator bias controller.

Among them, the optical carrier from TLS is modulated by the electrical LFM signal (in this article, the electrical LFM signal comes from MATLAB simulation). After the filter and amplifier, the light field can be written as:

$$E_o(t) = E_o \exp[i * (\omega_c t + \pi k t^2)] \qquad 0 \le t \le T$$

where E_o is the complex amplitude, ω_c is the frequency of the optical carrier, k is the chirp rate of the electrical LFM signal, and T is the pulse width of the electrical LFM signal. [25]

Therefore, the instantaneous optical frequency can be given by

$$\omega_o(t) = \omega_c + 2\pi k t$$

The instantaneous optical frequency of the propagated optical signal can be shown as

$$\omega_d(t) = \omega_c + 2\pi k\{t - \tau_1 - GD[\omega_d(t)]\}$$

Where τ_1 is the delay of the measurement path and GD(ω) is the group delay response of the DUT. Therefore, the propagated optical signal can be given by

$$E_d(t) = E_d A[\omega_d(t) \exp [i * \int \omega_d(t) dt]$$

where E_d is the complex amplitude of the optical signal injected into the DUT, A(ω) is the magnitude response of the DUT, and τ_1 + GD (ω_c) ≤ t ≤ τ_1 + T + GD (ω_c+2πkT). The next steps are similar to ordinary light vector analysis systems.

3. SIMULATION

3.1 The simulation of OVA based on ODSB

First, we constructed a detailed structure diagram according to the basic structure of the ODSB-based OVA in Figure 2 and built it in VPI Photonics. Figure 6 below shows the OVA structure diagram built in VPI Photonics.

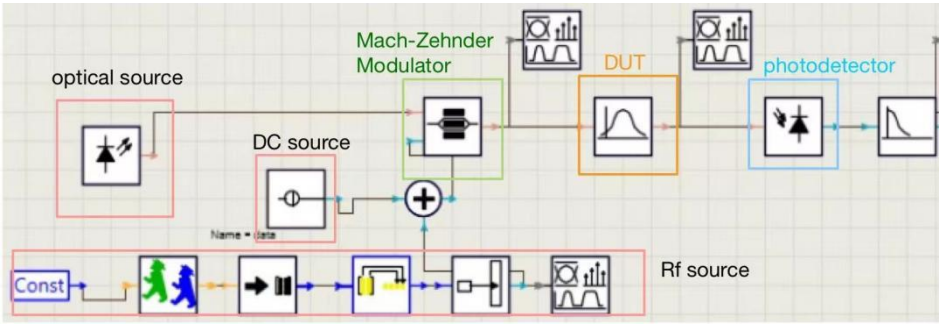

Figure 6. The structure of ODSB-based Optical vector analysis using VPI Photonics

As shown in the figure, the characteristic parameters of the optical system are: 1. Emission frequency of laser is 193.1e12Hz, average power 0.1W, and line width 1e6Hz. Extinction ratio of MZM is 30dB, symmetry factor is -1. Among them, DC source is used to control the MZM bias to maintain the minimum transmission point and suppress the power of the optical carrier as much as possible. The DUT is served by a bandpass filter (The bandwidth is 20GHz). The

responsivity of the PD is 1.0 A/W. The swept RF signal and subsequent amplitude and phase detection are jointly simulated by VPI Photonics and MATLAB.

Figure 7 below shows the ODSB spectrum generated with the 10GHz RF signal frequency.The power difference between the positive and negative first-order sidebands and the optical carrier is about 60dBm, so it can be regarded that the ODSB-based OVA is not affected by the optical carrier. We can observe the high-order sidebands in the figure because of the nonlinearity of the MZM, and their power is about 20dB smaller than the power of the required scanning sidebands (i.e., positive and negative first-order sidebands). Therefore, theoretically speaking, if you want to suppress the components generated by high-order sidebands in this system, you only need to use digital filtering to filter them out in the digital processing stage, so the errors caused by high-order sidebands can also be ignored. This issue will be simulated and demonstrated in detail in the next section.

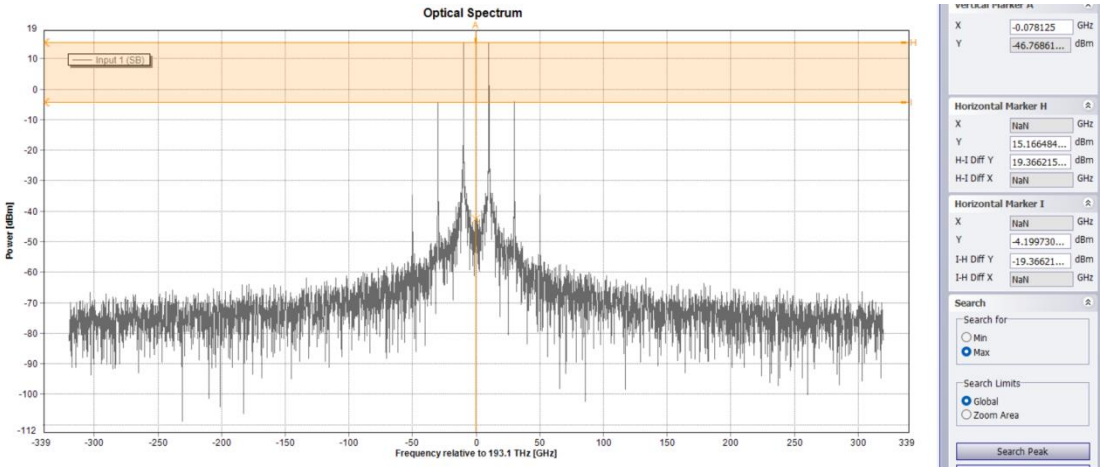

Figure 7. Optical spectrum of the modulated ODSB signal with a 10GHz RF signal.

Figure 8 shows the frequency response of the bandpass filter with a bandwidth of 20GHz measured by the built OVA. It can be seen that Figure 8(a) is the amplitude response of the DUT, which conforms to the frequency response of a Butterworth bandpass filter with a bandwidth of 20GHz. Figure 8(b) shows the phase response of the DUT.

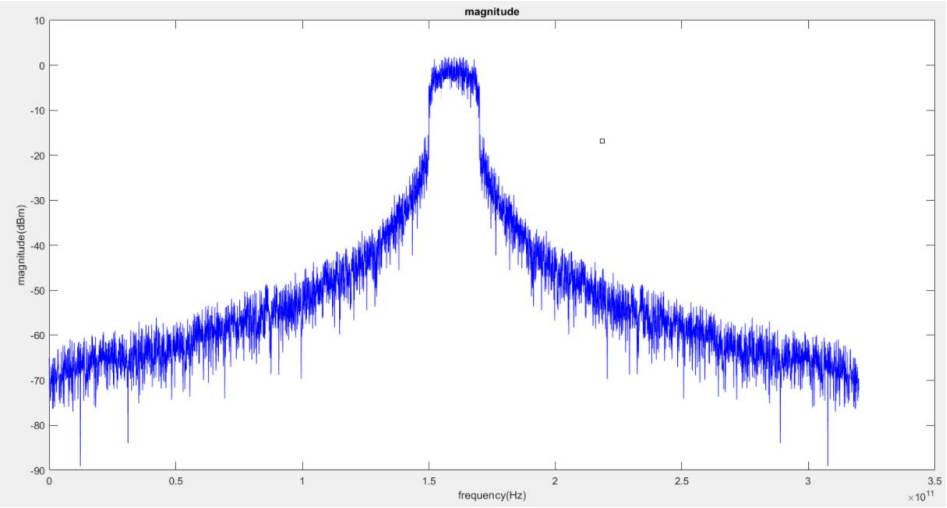

(a) The magnitude response measured with the proposed DUT

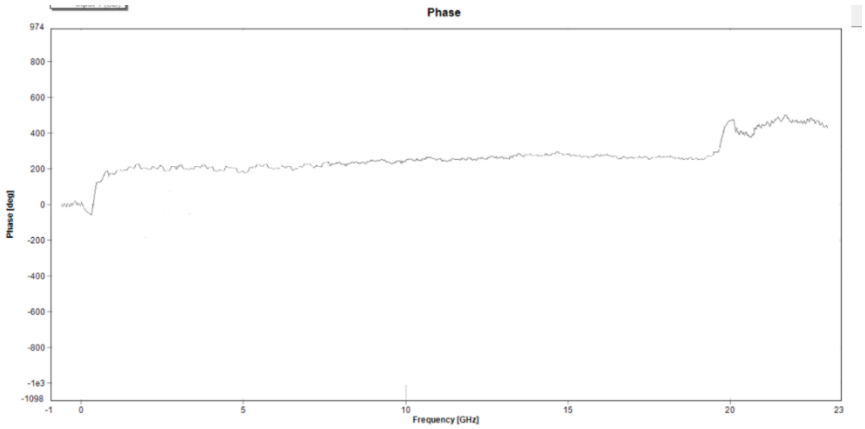

(b) The phase response measured with the proposed DUT

Figure 8. The amplitude and phase response of the bandpass filter with a bandwidth of 20GHz measured by the built ODSB-based OVA. The top figure is the magnitude response measured with the DUT. The bottom two figure shows the phase responses measured with the DUT.

Due to the limitation of symmetrical ODSB, the system needs to be tested twice to obtain its amplitude response. Because the frequency point 193.1THz is set as the centre frequency point, that is, 0Hz, the phase change points are at -10GHz and 10GHz.

Then, the established OVA simulation model needs to be numerically simulated and analysed to improve the performance, and analyze its measurement range, measurement speed and measurement error.

3.2 The simulation of measurement range broadening technology

We built detailed simulation system used for principle verification in figure 9, which contains devices similar to those shown in the structural diagram, an extremely narrow linewidth laser, OFC generator, mode selection module, modulated optical signal module and post-processing module. According to existing equipment, the linewidth of the laser is 300Hz.

In this simulation, the main equipment of the OFC generator is composed of a phase modulator, MZM and highly nonlinear optical fiber (1550 nm). The mode selection module consists of two tunable optical passband filters (OBPF). OBPF1 removes noise outside the passband, and its bandwidth is about 9nm. OBPF2 selects the nth comb line from OFC. The selected comb line enters the next stage as an optical carrier and is divided into two paths. Part of it passes through a frequency converter to shift the frequency of the optical carrier signal up by 80MHz. [22] The other part is used to form a carrier-suppressed ODSB modulation signal, which is modulated by a swept RF signal at another MZM. The optical carrier and optical double-sideband modulation signals are then combined to form an asymmetric optical signal for measurement. This system set up in Opti system.

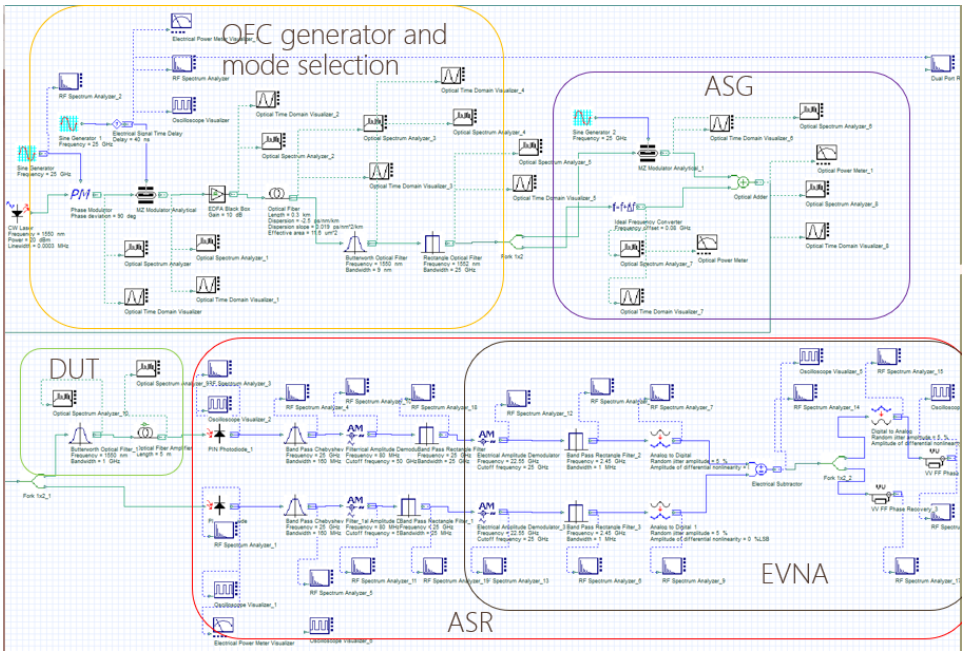

Figure 9. The simulation setup of the proposed OVA. ASG, asymmetric optical probe signal generator; ASR: asymmetric optical probe signal receiver.

The figure 10 shows the spectral pattern of the formed OFC and the information of the comb lines selected from the OFC using mode selection.The frequency interval of the comb teeth generated by this OFC generation scheme is 25GHz, and the number of available comb line is 21. It can be seen that the side mode suppression ratio (SMSR) of the middlemost comb line selected in OFC is 60.58 dB, and it is 33.74 dB in the edge area.

In order to verify the feasibility of the proposed OVA, a bandpass filter with a bandwidth of 300GHz will be measured, and the obtained amplitude and phase responses are shown in Figure 11 below. Only need one measurement because of asymmetric optical probe signal. The phase response has a delay than the amplitude response.

The measurement range of the expanded OVA is 20 times larger than that of the ODSB-based OVA under the same parameters. It can be seen that the essence of this expansion lies in the coverage area of the generated optical comb line. If more comb lines and OFCs with wider frequency intervals are used, the theoretically expanded measurement range can reach tens or even hundreds of THz. However, this approach also has some drawbacks. Under the study of Beha et al. [26], when performing signal modulation, the RF synthesizer generates phase noise, causing the linewidth of the comb

lines to broaden, which may lead to resolution degradation. That is, when expanding the measurement range, it is necessary to select a laser with a narrower linewidth as much as possible to ensure high resolution.

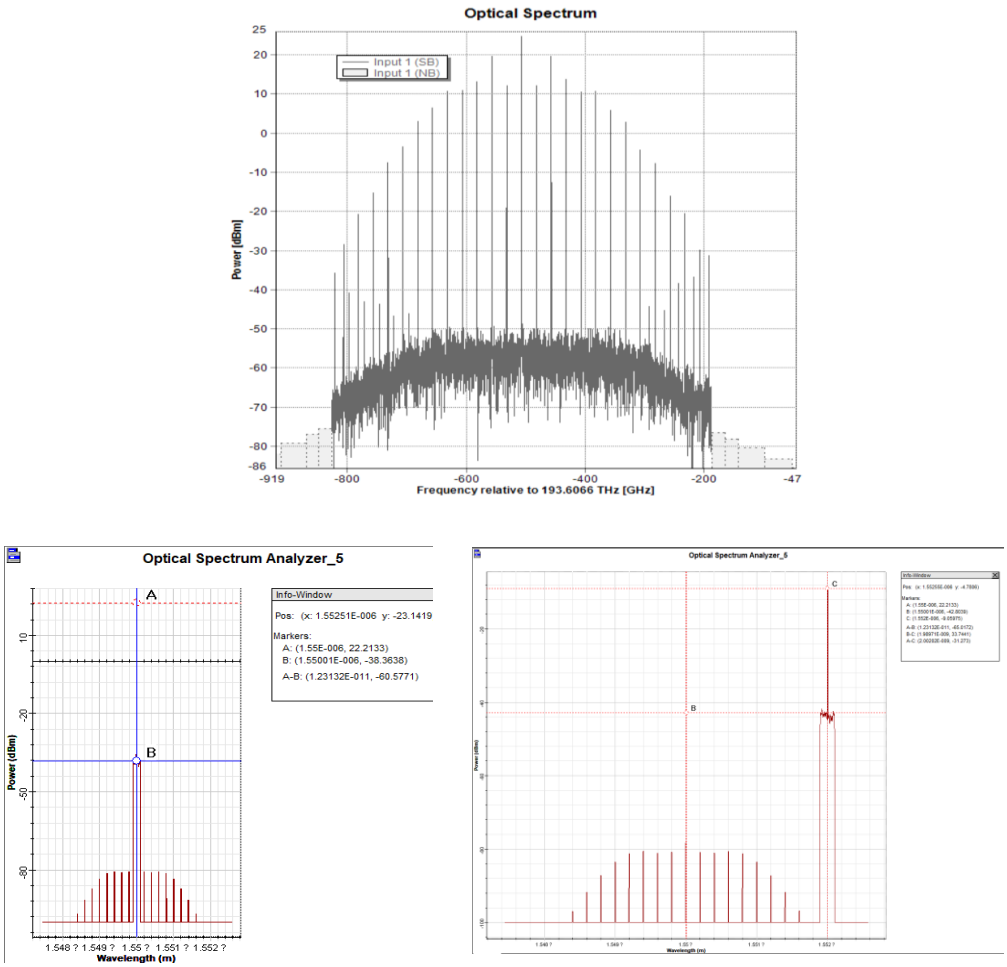

Figure 10. The optical spectral of the OFC and the selected comb line. The top figure: the generated 21-tone OFC signal. The bottom figure: the comb line in the middle(left) and marginal area(right) of the OFC selected by OBPF2.

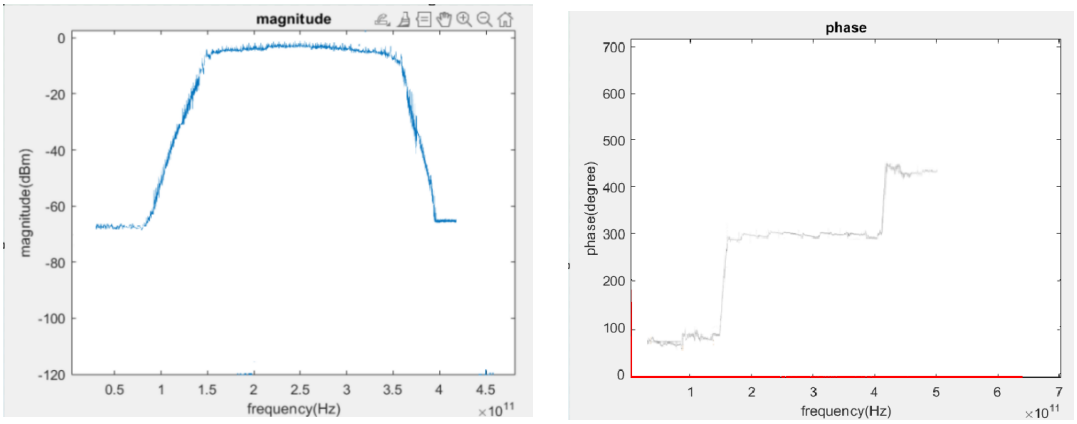

Figure 11. The amplitude and phase response of the bandpass filter (bandwidth of 300GHz) measured by the proposed OVA.

3.3 The simulation of nonlinear error analytical analysis, simulation and elimination

The following figure 12 illustrates the simulation diagram of OVA based on carrier suppression and balanced photodetection in VPI Photonics. The RF sweep source generated in MATLAB. The DUT is a bandpass filter, and its 3dB-bandwidth is 5GHz. And the other parameters are the same as them in ordinary ODSB-based OVA. Compared with the ordinary ODSB-based OVA, the frequency responses of them are in figure 13.

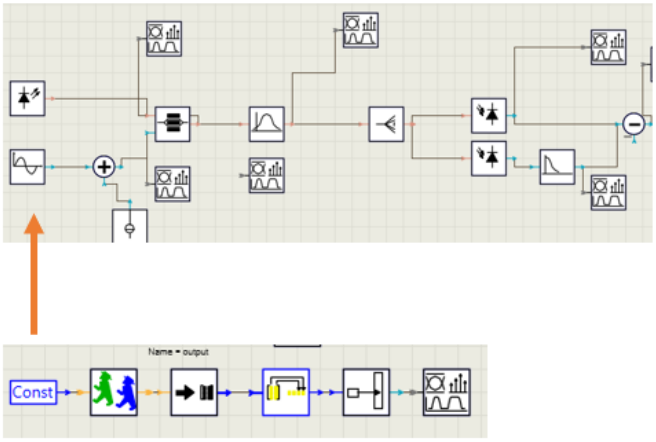

Figure 12. The simulation structure of OVA based on carrier suppression and balanced photodetection

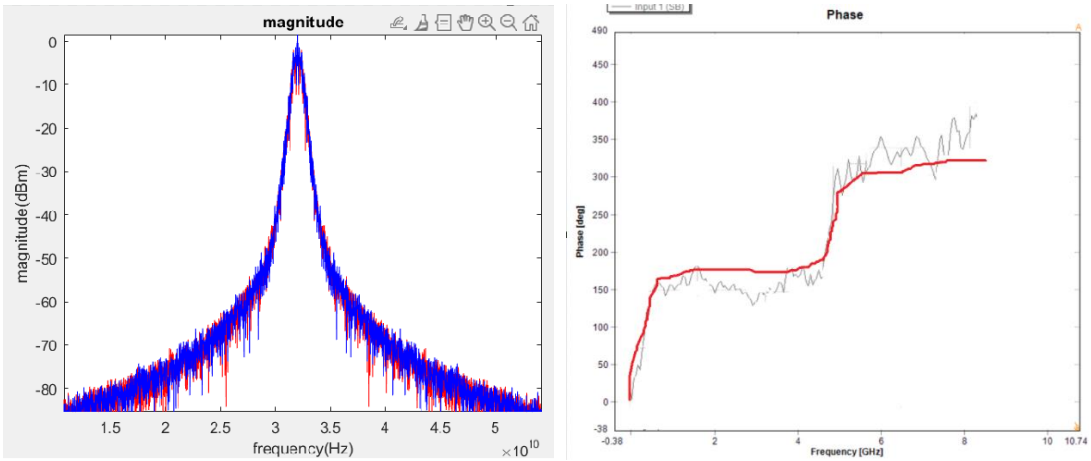

Figure 13. The amplitude (left figure: blue line is the proposed OVA, red line is the ordinary OVA) and phase(right figure: red line is the proposed OVA, black line is the ordinary OVA) response of the bandpass filter with a bandwidth of 5GHz measured by the proposed OVA and the ordinary OVA based on ODSB

It can be found that the performance has an obvious improvements, however, there is still a lot of noise in the amplitude response after elimination. The guess for this situation is that for OVA, the biggest influencing factor comes from the beat frequency of the negative first-order sideband with incomplete isolation.

Theoretically, if the two optical paths have the same length and loss, this error elimination method can completely suppress nonlinear errors. However, in actual measurement, the effect of temperature on the length of the optical fibers in the two optical paths and the imbalance of the balanced photodetector need to be considered.

3.4 The simulation of ultra-high resolution optical vector analysis based on LFM

The simulation was carried out based on the settings of the structure diagram. The simulation structure diagram is as follows.

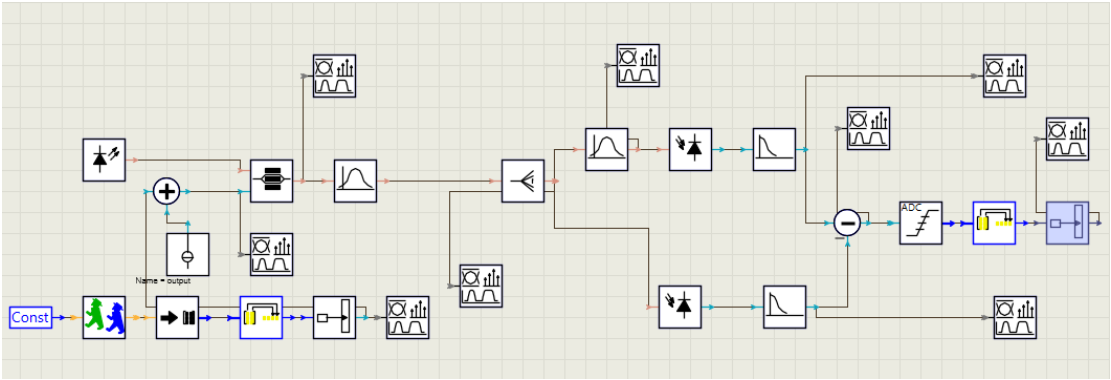

Figure. 14 The simulation structure diagram of ultra-high-resolution OVA based on LFM.

The optical carrier linewidth generated by TLS is less than 100kHz. MZM and bandpass filters are used to generate carrier suppressed OSSB modulators. MBC keeps the MZM bias at the minimum transmission point to suppress the carrier as much as possible. The pulse width of the electrical LFM signal is 10us. The DUT is acted by a filter with a bandwidth of 2GHz. Finally, the photocurrent from the BPD is sampled with a sampling power of 1GS/s.

The LFM signal is generated by MATLAB with a bandwidth of 16GHz, a chirp frequency of 1600THz/s, and a sampling rate of 64GS/s. The figure shows the magnitude and phase response as follows:

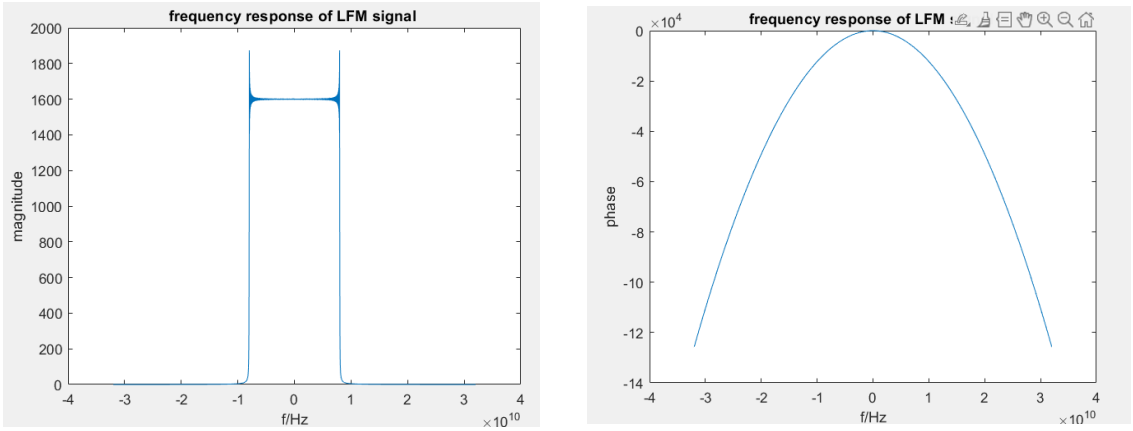

Figure.15 The magnitude(left) and phase(right) response of LFM signal

The following figure 16 shows the amplitude and phase response of the bandpass filter with a bandwidth of 2 GHz. Compared with OSSB-based OVA, when using the same system and the same parameters, the LFM-based OVA only need 4m,16s. But the OSSB-based OVA needs 9m,20s in simulation with computer. The maximum insertion loss of the measured magnitude response shown in Fig is about 50 dB.

Theoretically, due to the extremely narrow pulse width, the system measurement time based on optical LFM signals is only 10 μs. Due to the advantage of fast measurement time, LFM-based OVA is insensitive to temperature changes and mechanical vibrations. Although the measurement theoretical resolution is affected by the measurement time, due to the linear time-frequency characteristics of the LFM signal, the frequency resolution of the proposed LFM-based OVA will be the signal bandwidth divided by the total number of sampling points. The simulation measurement time in this article is 10μs, and the calculated measurement resolution is 1.6MHz (16GHz/1GS/s×10μs).

The resolution also depends on the sweep frequency point of the LFM signal. Because the scanning speed is very fast, the sweep frequency point can be increased according to needs.

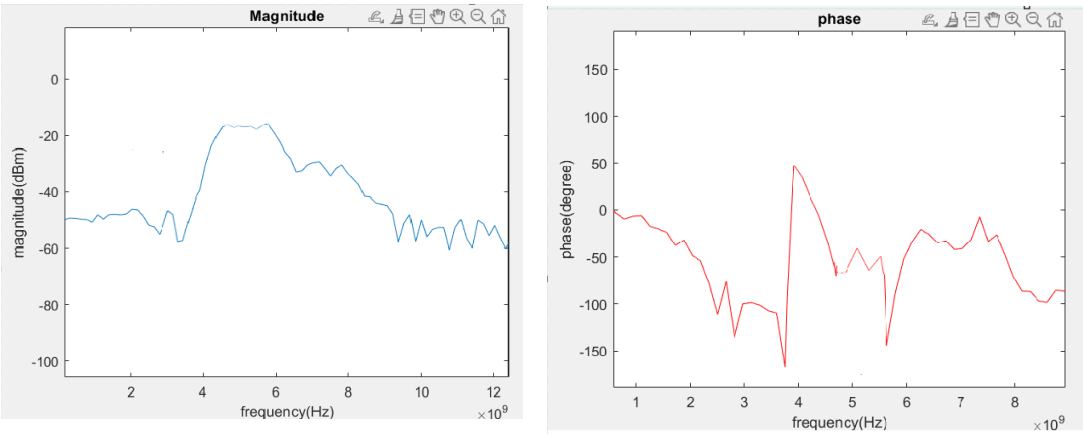

Figure.16 The amplitude and phase response of the bandpass filter with a bandwidth of 2GHz measured by the proposed OVA.

4. CONCLUSION

1. We conducted in-depth research on Microwave spectrum analysis in microwave photon measurement to understand the principles and structures of optical vector analysis.

2. Conducted detailed research and simulation on OVA based on ODSB, and optimized and expanded it.

A. Measurement range expansion technology based on optical frequency comb. With the support of this technology, the measurement range of tens of GHz can be expanded to hundreds of GHz or even THz. In this article, we expanded the range in 20 times larger, and can flexibly change the measurement range by changing the number and spacing of OFC comb lines. Therefore, when we need to measure a device with unknown parameters, we can first increase the number and spacing of comb lines to perform rough measurements to determine its spectrum, and then narrow the measurement range and perform fine measurements by reducing the number and spacing of comb lines.

B. Error elimination technology based on carrier suppression and balanced photodetectors reduces measurement errors caused by high-order sidebands to a certain extent. However, there are still errors in the measured frequency response results, which is caused by incomplete isolation of the negative first-order sidebands during the measurement process. Overall, these two methods have improved the performance of OVA to a certain extent.

C. At the same time, LFM-based OVA is used to increase the measurement speed. Based on the characteristics of high LFM signal resolution, bandwidth and time width can be set by yourself, the proposed OVA can complete ultra-fast measurement and ultra-high-resolution measurement.

ACKNOWLEDGEMENTS

Sincerely express my gratitude to my supervisor, Professor Yu Changyuan., and he provided me with guidance on the topic and content of my dissertation. In addition, thanks for the guidance and idea from Dr. Zhong Kangping.

REFERENCES

[1] LI Shu-peng, QING Ting, WANG Li-hua, et al, "Optical vector analyzer with time-domain analysis capability," Opt Lett, 2021, 46(2): 186-189.

[2] CHEN Wei, XUE Min, ZHU Dan, et al. "Optical vector analysis with improved accuracy and enhanced dynamic range," IEEE Photonics Technol Lett, 2019, 31(19): 1565-1568.

[3] XUE Min, CHEN Wei, ZHU Dan, et al. "High-resolution optical vector network analyser employing optical double-sideband modulation and optical Hilbert transform," Electron Lett, 2019, 55(6): 337-338.

[4] WANG Bin, ZHANG Wei-feng, ZHAO Shuang-xiang, FAN Xin-yu. "Recent Progress in Microwave Photonic Sensors," Acta Electronica Sinica, 2022, 50(4): 769-781 https://doi.org/10.12263/DZXB.20211186.

[5] J. Capmany, J. Mora, I. Gasulla, J. Sancho, J. Lloret and S. Sales, "Microwave Photonic Signal Processing," in Journal of Lightwave Technology, vol. 31, no. 4, pp. 571-586, Feb.15, 2013, doi: 10.1109/JLT.2012.2222348.

[6] J. Yao, "Photonics to the Rescue: A Fresh Look at Microwave Photonic Filters," in IEEE Microwave Magazine, vol. 16, no. 8, pp. 46-60, Sept. 2015, doi: 10.1109/MMM.2015.2441594.

[7] J. Capmany, B. Ortega, and D. Pastor, "A tutorial on microwave photonic filters," J. Lightwave Technol. 24(1), 201–229 (2006).

[8] J. Mora, M. V. Andrés, J. L. Cruz, B. Ortega, J. Capmany, D. Pastor, and S. Sales, "Tunable all-optical negative multitap microwave filters based on uniform fiber Bragg gratings," Opt. Lett. 28(15), 1308–1310 (2003).

[9] F. Zeng, J. Wang, and J. P. Yao, "All-optical microwave bandpass filter with negative coefficients based on a phase modulator and linearly chirped fiber Bragg gratings," Opt. Lett. 30(17), 2203–2205 (2005).

[10] C. Wang and J. P. Yao, "Chirped microwave pulse compression using a photonic microwave filter with a nonlinear phase response," IEEE Trans. Microw. Theory Tech. 57(2), 496–504 (2009).

[11] Chao Wang and Jianping Yao, "Fiber Bragg gratings for microwave photonics subsystems," Opt. Express 21, 22868-22884 (2013)

[12] Zou, Xihua, Bing Lu, Wei Pan, Lianshan Yan, Andreas Stöhr, and Jianping Yao. "Photonics for microwave measurements," Laser & Photonics Reviews 10, no. 5 (2016): 711-734.

[13] M. Pelusi, F. Luan, T. D. Vo, M. R. Lamont, S. J. Madden, D. A. Bulla, D. Y. Choi, B. Luther-Davies, and B. J. Eggleton, "Photonic-chip-based radio-frequency spectrum analyzer with ter ahertz bandwidth," Nature Photon. 3(3), 139–143 (2009).

[14] Morozov, Oleg, Ilnur Nureev, Airat Sakhabutdinov, Artem Kuznetsov, Gennady Morozov, German Il'in, Samvel Papazyan, Alexander Ivanov, and Roman Ponomarev. "Ultrahigh-resolution optical vector analyzers," In Photonics, vol. 7, no. 1, p. 14. MDPI, 2020.

[15] H. Chi, X. Zou, and J. Yao. "An approach to the measurement of microwave frequency based on optical power monitoring," IEEE Photon. Technol. Lett. 20(14), 1249–1251 (2008).

[16] G. H. Smith, D. Novak, and Z. Ahmed. "Overcoming chromatic-dispersion effects in fiber-wireless systems incorporating external modulators," IEEE Trans. Microw. Theory Techn. 45(8), 1410–1415 (1997).

[17] M. T. de Melo, B. G. M. de Oliveira, I. Llamas-Garro, and M. Espinosa-Espinosa, "Radio frequency identification from system to applications," Ch. 14, (InTech, 2013).

[18] J. Beas, G. Castanon, I. Aldaya, A. Aragon-Zavala and G. Campuzano, “Millimeter-Wave Frequency Radio over Fiber Systems: A Survey,” in IEEE Communications Surveys & Tutorials, vol. 15, no. 4, pp. 1593-1619, Fourth Quarter 2013, doi: 10.1109/SURV.2013.013013.00135.
[19] Marpaung, D., Yao, J. & Capmany, J. “Integrated microwave photonics,” Nature Photon 13, 80–90 (2019). https://doi.org/10.1038/s41566-018-0310-5
[20] Marpaung, David, Chris Roeloffzen, René Heideman, Arne Leinse, Salvador Sales, and José Capmany. “Integrated microwave photonics,” Laser & Photonics Reviews 7, no. 4 (2013): 506-538.
[21] M. Xue, S. Liu and S. Pan, “High-Resolution Optical Vector Analysis Based on Symmetric Double-Sideband Modulation,” in IEEE Photonics Technology Letters, vol. 30, no. 5, pp. 491-494, 1 March1, 2018, doi: 10.1109/LPT.2018.2799565.
[22] Qing, T., Li, S., Tang, Z., Gao, B., & Pan, S. (2019). “Optical vector analysis with attometer resolution, 90-dB dynamic range and THz bandwidth,” Nature communications, 10(1), 5135
[23] Xue, Min, Shilong Pan, Chao He, Ronghui Guo, and Yongjiu Zhao. “Wideband optical vector network analyzer based on optical single-sideband modulation and optical frequency comb,” Optics Letters 38, no. 22 (2013): 4900-4902.
[24] Xue, Min, Yongjiu Zhao, Xiaowen Gu, and Shilong Pan. “Performance analysis of optical vector analyzer based on optical single-sideband modulation,” JOSA B 30, no. 4 (2013): 928-933.
[25] Li, Shupeng, Min Xue, Ting Qing, Changyuan Yu, Lugang Wu, and Shilong Pan. “Ultrafast and ultrahigh-resolution optical vector analysis using linearly frequency-modulated waveform and dechirp processing,” Optics Letters 44, no. 13 (2019): 3322-3325.
[26] Beha, Katja, Daniel C. Cole, Pascal Del’Haye, Aurélien Coillet, Scott A. Diddams, and Scott B. Papp. “Electronic synthesis of light,” Optica 4, no. 4 (2017): 406-411.